Geosciences and Engineering, Vol. 14, No. 1 (2026), pp. 61–73.
https://doi.org/10.33030/geosciences.2026.01.005

REFERENCE-BASED MEASUREMENT OF STRESS-DEPENDENT ULTRASONIC VELOCITY AND SEISMIC QUALITY FACTOR

BRIGITTA TURAI-VUROM[1]*, MIHÁLY DOBRÓKA[2]
[1]**Institute of Exploration Geosciences, University of Miskolc; brigitta.vurom@gmail.com*
[2]*Institute of Exploration Geosciences, University of Miskolc; dobrokam48@gmail.com*
[1]*https://orcid.org/0000-0001-7483-6458*
[2]*https://orcid.org/0000-0003-3956-2070*

Abstract: We report ultrasonic laboratory measurements of P-wave velocity and quality factor (Q) in a sandstone sample under stepwise uniaxial loading (0–90 kN). Full ultrasonic waveforms were recorded at each load increment. Because Q estimation is more sensitive than velocity to coupling conditions, instrumental response, and spectral processing, particular emphasis was placed on amplitude-consistent acquisition and reference-based attenuation analysis. An aluminum specimen of identical geometry was measured under the same protocol to characterize system-related attenuation and to enable spectral-ratio-based estimation of effective Q relative to a high-Q reference. The sandstone exhibits pronounced stress dependence in both velocity and Q, indicating path-dependent anelastic dissipation associated with microcrack closure and frictional grain-contact losses.

***Keywords**: stress-dependence, Q-factor, measurement methodology, spectral-ratio, geophysical inversion*

1. INTRODUCTION

The propagation characteristics of seismic waves provide valuable information about the fundamental mechanical properties of rocks. For this reason, determining the velocity and attenuation of acoustic waves is a common task in laboratory experiments. Over several decades, numerous researchers have examined the velocity of acoustic waves traveling through various rock types under different confining pressure conditions (Wyllie et al. 1958; Stacey 1976; King 2009), as well as under varying pore pressure levels (Nur and Simmons 1969; Darot and Reuschlé 2000; He and Schmitt 2006). It has long been recognized that wave velocity increases with increasing stress, a phenomenon that has been discussed and interpreted in several rock mechanics studies (Wyllie et al. 1956; Birch 1960). One of the most widely accepted explanations attributes this effect to the closure of microcracks within rocks when pressure increases (Best 1997; Hassan and Vega 2011; Sengun et al. 2011).

Seismic and ultrasonic attenuation, commonly described by the quality factor Q, provides information complementary to velocity by constraining anelastic and dissipative behavior of rocks (Toksöz and Johnston 1981; Mavko et al. 2009). Pressure-dependent velocity variations are widely attributed to the progressive closure of compliant pores and microcracks, while attenuation often decreases with increasing

stress as these features close and frictional losses diminish (Toksöz et al. 1979; Meglis et al. 1996). However, laboratory studies that document attenuation during loading cycles are still less common, and disentangling intrinsic rock losses from system- and coupling-related effects remains challenging, because determining Q is a more challenging and complex task than determining acoustic velocity. In contrast to first arrival-based velocity estimation, Q-factor determination is highly sensitive to the details of the measurement chain and data processing. Whereas velocity can often be obtained from a relatively robust travel-time pick, attenuation estimation requires stable source conditions, repeatable transducer coupling, gain-corrected amplitudes, careful waveform windowing, appropriate frequency-band selection, and separation of intrinsic rock losses from instrumental and interface-related effects. Consequently, reliable Q estimation is not only a petrophysical problem but also a measurement-technology problem, and the experimental protocol must be designed accordingly.

Here we present ultrasonic measurements on a sandstone sample under stepwise loading and quantify the stress dependence of both wave velocity and Q. To isolate intrinsic attenuation, we perform identical measurements on an aluminum specimen of the same geometry, used as a high-Q reference, consistent with spectral-ratio approaches commonly used in pulse-transmission experiments (Toksöz et al. 1979; Zong et al. 2020). Such coupled velocity–attenuation investigations can provide direct laboratory evidence that attenuation is more sensitive to stress history than elastic stiffness alone.

2. Samples and Experimental Setup

2.1. Sandstone sample

To investigate stress-dependent ultrasonic properties, a cylindrical sandstone sample was prepared and characterized prior to the experimental measurements. The sandstone sample has length L = 6.95 cm and diameter D = 3.79 cm. The dry mass is 191.06 g and the helium porosity is 11.5%. The sample originates from a Hungarian oil field at a depth of 1822.50–1822.60 m.

2.2. Aluminum reference sample

An aluminum specimen with identical geometry was used as a reference to quantify instrumental and coupling-related attenuation. Because aluminum exhibits a high Q at ultrasonic frequencies compared with most sedimentary rocks, it provides a practical baseline for spectral-ratio-based attenuation estimation relative to a reference sample (Toksöz et al. 1979; Zong et al. 2020).

2.3. Loading protocol and acquisition

The pulse transmission method (Toksöz et al. 1979) was applied to determine the acoustic wave velocities. The experimental apparatus is in the Acoustic Laboratory

of the Department of Geophysics, University of Miskolc. The experimental setup is shown in Figure 1.

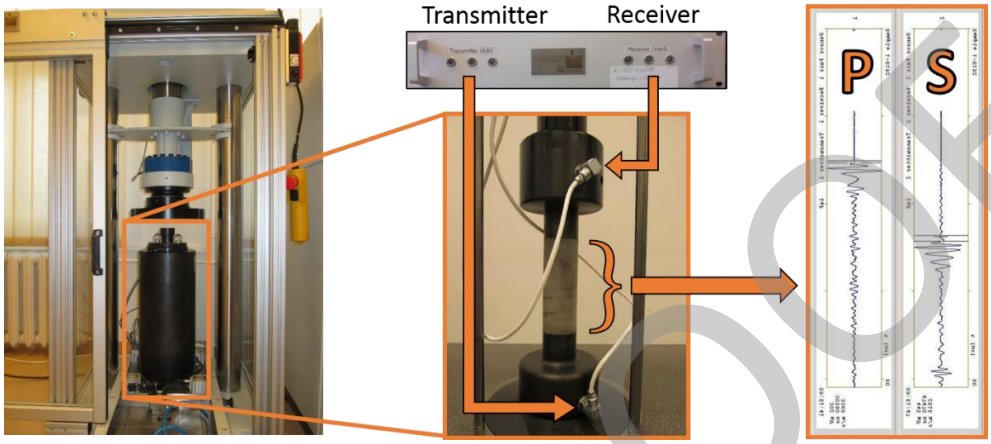

Figure 1

Experimental setup. Left: pressure cell and load frame. Middle: sandstone sample between transmitter and receiver (built-in pressure stamps). Right: Typical P and S wave arrivals

The digitally controlled measuring system includes a pressure vessel, a load frame, a pressure generator that ensures mantle pressure, and a two-channel acoustic measuring instrument connected to these, as well as software that controls the above and performs ultrasonic velocity measurements. The laboratory system is capable of both confining-pressure and axial-loading experiments; however, in the present study only the axial loading branch was used. The rock specimen was examined under uniaxial loading using an electromechanical press, and the wave velocities were recorded as a function of applied axial stress at successive stress levels.

At each load step, full waveforms containing P- and S-wave arrivals were recorded; in the present work, we analyze the P-wave portion. Measurements were performed using piezoelectric transducers with central frequency 0.5 MHz. Waveforms were recorded from 0.01 to 90 μs at a 0.01 μs sampling interval. To increase the signal-to-noise ratio, we used 256-fold vertical summation, which means averaging 256 consecutive measurements in the instrument's memory. This method significantly reduced the amplitude of external noise in the displayed waveform. The applied load was increased stepwise from 0 to 90 kN.

These acquisition details are particularly important for attenuation analysis. In velocity measurements, the principal observable is the arrival time, but Q estimation depends on the spectral amplitudes of the recorded waveform and is therefore much more sensitive to coupling variations, instrumental response, signal-to-noise ratio, and processing choices. For this reason, waveform repeatability and amplitude-consistent acquisition were treated as critical requirements of the experiment.

3. DATA PROCESSING AND Q ESTIMATION

Although velocity and attenuation are derived from the same ultrasonic recordings, the two estimations differ substantially in methodological complexity. Velocity is determined from a first-arrival pick, whereas Q estimation requires additional amplitude-preserving processing and spectral modeling. Therefore, the attenuation workflow is more sensitive to experimental uncertainty than the velocity workflow.

3.1. P-wave velocity

At each load step, the P-wave first-arrival time was picked from the recorded waveform. The P-wave velocity was computed as $vp = L / tp$, where L is the specimen length and tp is the first-arrival travel time.

3.2. Waveform conditioning for spectral analysis

Raw waveform data were converted, and amplitudes were corrected for the acquisition gain. For spectral analysis, each trace was trimmed so that the time series begins at the first arrival, removing the pre-arrival segment. A constant offset was removed by subtracting the mean of the trimmed signal from each sample to prevent introducing a strong DC component in the Fourier spectrum. Discrete Fourier transforms were then computed using custom MATLAB code.

3.3. Spectral ratio method with aluminum reference

Reliable attenuation analysis requires amplitude-consistent data processing and careful correction of system-related effects. In the present study, this was achieved by applying a reference-based spectral-ratio approach using an aluminum specimen measured under identical experimental conditions.

In the frequency domain, the recorded ultrasonic signal can be expressed as a product of source, coupling, transmission, and attenuation terms

$$U(\omega) = F(\omega)\, C(\omega)\, G(l)\, A(\omega,l) \tag{1}$$

where $U(\omega)$ is the complex spectrum of the recorded signal, $F(\omega)$ is the source spectrum, $C(\omega)$ is the frequency-dependent coupling factor, $G(l)$ represents the propagation and geometrical transfer effects, and $A(\omega,l)$ describes attenuation along the travel path of length l. For the sandstone specimen and the aluminum reference sample measured under identical experimental conditions, the spectra can be written as $U_R(\omega) = F(\omega)\, C(\omega)\, G_R(l)\, A_R(\omega,l)$ and $U_A(\omega) = F(\omega)\, C(\omega)\, G_A(l)\, A_A(\omega,l)$, where the subscripts R and A refer to the rock and aluminum samples, respectively. Their ratio can be given as

$$\frac{U_R(\omega)}{U_A(\omega)} = \frac{F(\omega)C(\omega)G_R(l)\,A_R(\omega,l)}{F(\omega)C(\omega)G_A(l)A_A(\omega,l)} = \frac{G_R(l)}{G_A(l)}\frac{e^{-a_R l}}{e^{-a_A l}} = \frac{G_R(l)}{G_A(l)}e^{-(a_R-a_A)l} \tag{2}$$

and

$$a = \frac{\omega}{2vQ} = \frac{\pi f}{v}\frac{1}{Q} \tag{3}$$

where *a* is attenuation, *v* denotes the velocity measured in m/s, and *Q* represents the quality factor. Thus,

$$ln\frac{U_R(\omega)}{U_A(\omega)} = ln\frac{G_R(l)}{G_A(l)} - (a_R - a_A)l = ln\frac{G_R(l)}{G_A(l)} - \pi f\left(\frac{1}{Q_R v_R} - \frac{1}{Q_A v_A}\right)l =$$

$$ln\frac{G_R(l)}{G_A(l)} - \pi f\left(\frac{1}{Q_R}\frac{l}{v_R} - \frac{1}{Q_A}\frac{l}{v_A}\right) = ln\frac{G_R(l)}{G_A(l)} - \gamma * f \tag{4}$$

Since the term $\frac{G_R(l)}{G_A(l)}$ is independent of frequency (Toksöz et al. 1979), the γ slope can be determined from the line as follows

$$\gamma = \pi\left(\frac{\Delta t_R}{Q_R} - \frac{\Delta t_A}{Q_A}\right). \tag{5}$$

The quality factor of the aluminium Q_A is much higher than that of the rock, therefore to a good approximation

$$\gamma \approx \pi\frac{\Delta t_R}{Q_R}, \tag{6}$$

giving

$$Q_R = \pi\frac{\Delta t_R}{\gamma}. \tag{7}$$

Following the above procedure, the amplitude spectrum was computed from the Fourier transform of the conditioned P-wave time series. Let $A_R(f, P)$ denote the sandstone amplitude spectrum and $A_A(f, P)$ the aluminum reference spectrum at frequency *f* and applied load *P*. The spectral ratio $R(f, P) = A_R(f, P) / A_A(f, P)$ was formed and its natural logarithm $ln\ R(f, P)$ was taken.

Under the standard pulse-transmission attenuation model, the logarithm of the spectral ratio is approximately linear in frequency over a selected band, with slope proportional to travel time and reciprocal value of Q (Toksöz et al. 1979):

$$ln\ R(f, P) \approx C(P) - (\pi f\, t(P)) / Q(P) \tag{8}$$

where $t(P)$ is the P-wave travel time through the sandstone at load level *P* and $C(P)$ absorbs frequency-independent factors such as coupling and source amplitude differences. $Q(P)$ was estimated by linear regression of $ln\ R$ versus *f* over the frequency

band 4–96 kHz, corresponding to the effective bandwidth of the recorded signal after windowing. Because the reference specimen has high Q, this procedure yields an estimate of the sandstone's effective (path-averaged) Q_P at each load step, after removing much of the instrumental response (Toksöz et al., 1979; Zong et al., 2020).

In the following, Q_P denotes the effective, path-averaged P-wave quality factor estimated from spectral ratios between the sandstone and aluminum reference samples, representing intrinsic anelastic attenuation within the selected frequency band. Figure 2 shows the spectral ratio between the sandstone and the aluminum reference sample as a function of frequency, from which the slope used for Q estimation is derived.

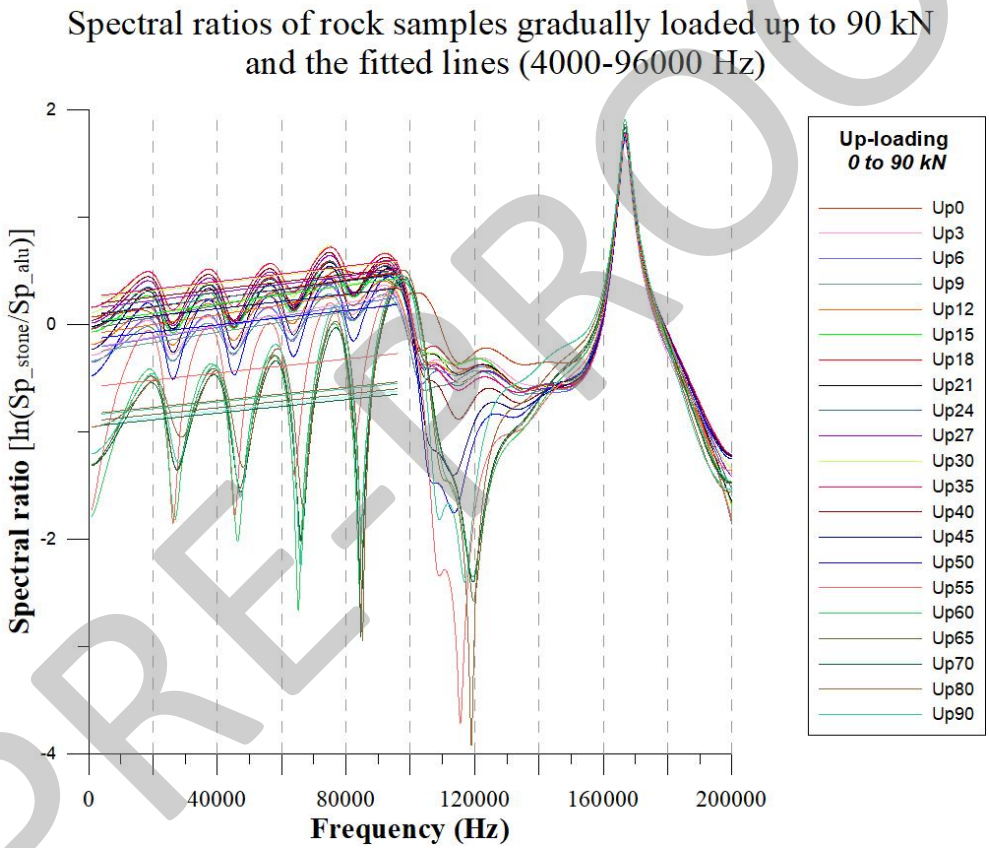

Figure 2

Spectral ratio as a function of frequency

3.4. Inversion methodology

The stress dependence of both P-wave velocity and quality factor was further analyzed by nonlinear inversion. The inversion was performed using a physically moti-

vated parametric model describing the stress-induced evolution of elastic and anelastic properties. Separate model functions were defined for the velocity and quality factor branches, allowing the stress-dependent behavior to be captured explicitly.

The inversion was formulated as a nonlinear least-squares optimization problem, in which model parameters were estimated by minimizing the misfit between the observed data and the model predictions (Dobróka and Somogyiné Molnár, 2012b). In this framework, the number of observations exceeds that of the unknowns, allowing stable parameter estimation without strong regularization.

Let $d_{obs}(P_i)$ denote the measured data (either velocity or Q factor) at the i-th stress level P_i, and let $d_{calc}(P_i, \mathbf{m})$ denote the corresponding model response, where $\mathbf{m}$ is the vector of model parameters. The inversion aims to minimize the following objective function:

$$\Phi(\mathbf{m}) = \sum_{i=1}^{N}[d_{obs}(P_i) - d_{calc}(P_i, \mathbf{m})]^2 \tag{9}$$

This objective function represents the squared L_2-norm of the data misfit. The forward problem is defined by nonlinear model functions describing the stress dependence of velocity and quality factor:

$$v(P) = f(P, \mathbf{m}_v) \tag{10}$$

$$Q(P) = g(P, \mathbf{m}_Q) \tag{11}$$

The minimization was carried out using an iterative linearization approach. At each iteration step k, the forward problem was linearized using a first-order Taylor expansion:

$$\mathbf{d}_{calc}(\mathbf{m}_k + \Delta\mathbf{m}) \approx \mathbf{d}_{calc}(\mathbf{m}_k) + \mathbf{J}(\mathbf{m}_k)\Delta\mathbf{m} \tag{12}$$

where $\mathbf{J}$ is the Jacobian matrix of partial derivatives.

$$(\mathbf{J}^T\mathbf{J})\,\Delta\mathbf{m} = \mathbf{J}^T[\mathbf{d}_{obs} - \mathbf{d}_{calc}(\mathbf{m}_k)] \tag{13}$$

$$\mathbf{m}_{k+1} = \mathbf{m}_k + \Delta\mathbf{m} \tag{14}$$

The iteration continued until convergence was achieved.

The inversion algorithm was implemented in MATLAB and is based on the nonlinear inversion framework developed by Dobróka and Somogyiné Molnár (2012b), widely applied in geophysical parameter estimation and rock physics modeling. The method allows stable estimation of model parameters even in the presence of nonlinear relationships and limited data.

The resulting inverted model curves provide a physically consistent description of the observed velocity–stress and Q_P–stress relationships and are shown as solid lines in Figures 3 and 4.

4. RESULTS

Measurements were conducted under stepwise uniaxial loading between 0 and 90 kN. The applied axial force was converted to axial stress using the sample cross-sectional area, yielding the following stress levels: 0.22, 2.66, 5.33, 7.99, 10.66, 13.32, 15.99, 18.65, 21.32, 23.98, 26.65, 31.09, 35.53, 39.97, 44.41, 48.86, 53.30, 57.74, 62.18, 71.06, 79.95 MPa (after converting the values measured in kN to MPa). The corresponding measured velocities and estimated Q values for each stress level are summarized in Table 1.

Table 1
Measured and calculated data

Load (kN)	Pressure (MPa)	First arrival time (μs)	Velocity (m/s)	Equation of linear regression	Q
0.25	0.222	13.55	5127.7	5.628E-006 * X - 0.0496	75.599
3	2.665	13.44	5169.6	5.3073E-006 * X - 0.2264	79.519
6	5.330	13.36	5200.6	5.021E-006 * X - 0.2305	83.543
9	7.995	13.3	5224.1	4.796E-006 * X - 0.2676	87.073
12	10.659	13.25	5243.8	4.613E-006 * X - 0.0973	90.196
15	13.324	13.21	5259.7	4.345E-006 * X + 0.0124	95.471
18	15.989	13.185	5269.6	4.192E-006 * X + 0.0756	98.809
21	18.654	13.16	5279.6	4.027E-006 * X + 0.0817	102.605
24	21.319	13.14	5287.7	3.905E-006 * X + 0.0865	105.657
27	23.984	13.13	5291.7	3.777E-006 * X + 0.1444	109.155
30	26.648	13.11	5299.8	3.679E-006 * X + 0.2340	111.904
35	31.090	13.09	5307.9	3.584E-006 * X + 0.2533	114.696
40	35.531	13.07	5316.0	3.493E-006 * X + 0.1839	117.500
45	39.973	13.045	5326.2	3.406E-006 * X + 0.0069	120.311
50	44.414	13.035	5330.3	3.348E-006 * X - 0.1411	122.313
55	48.855	13.02	5336.4	3.267E-006 * X - 0.5870	125.141
60	53.297	13.007	5341.7	3.235E-006 * X - 0.9350	126.288
65	57.738	12.99	5348.7	3.168E-006 * X - 0.9059	128.763
70	62.179	12.975	5354.9	3.138E-006 * X - 0.9548	129.791
80	71.062	12.96	5361.1	3.111E-006 * X - 0.8370	130.824
90	79.945	12.95	5365.3	3.101E-006 * X - 0.8502	131.143

4.1. Velocity vs. stress model

The variation of P-wave velocity with increasing axial stress is shown in Figure 3. The measured data display a nonlinear increasing trend, with a relatively stronger increase at lower stress levels and a more gradual variation at higher stresses, the velocity increases nonlinearly with axial stress. This behavior is consistent with the progressive closure of compliant pores and microcracks during loading.

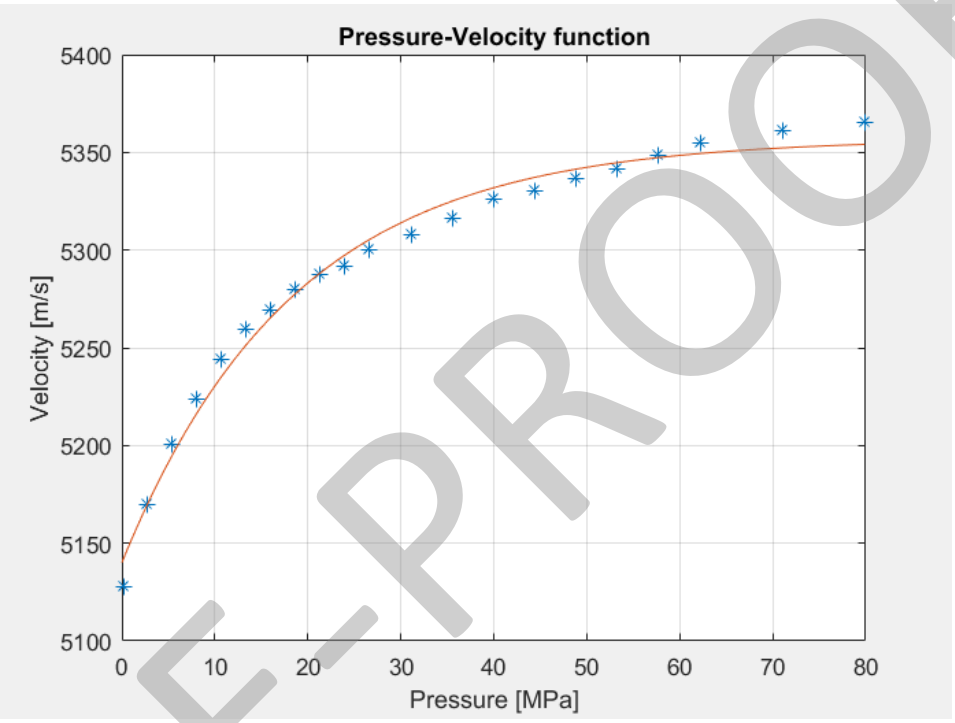

Figure 3

Stress dependence of P-wave velocity. The solid red line shows the curve derived from the fitted model obtained by nonlinear inversion and the blue stars indicate the measured velocity data

4.2. Q factor vs. stress model

The stress dependence of the effective P-wave quality factor is presented in Figure 4, the quality factor generally increases with stress, indicating reduced attenuation at higher stress levels. The estimated Q values generally increase with increasing axial stress, indicating reduced attenuation as compliant structural features progressively close. The final inversion resulted in a data distance of 0.93, which indicates that the proposed model adequately captures the stress-dependent evolution of the effective P-wave quality factor. Overall, the proposed relationship captures the main trend of the stress-dependent evolution of the effective P-wave quality factor.

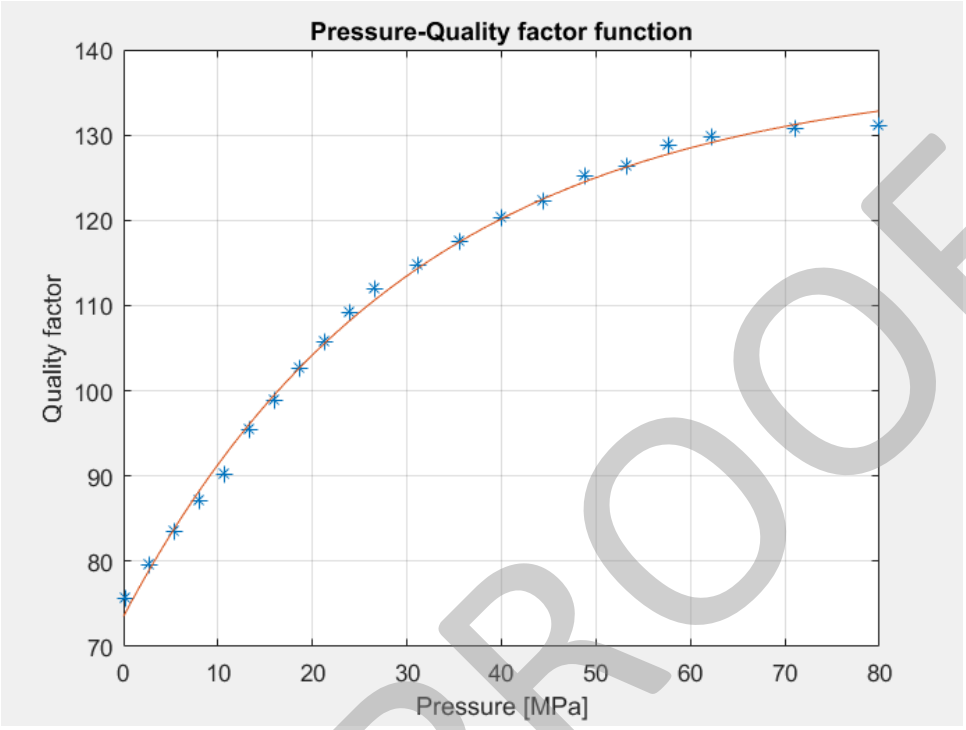

Figure 4

Stress dependence of the P-wave quality factor Q_P for the sandstone. Solid red line represents the model-derived curve and the blue stars indicate the calculated Q data

5. DISCUSSION

The results reveal systematic stress-dependent variations in both ultrasonic velocity and attenuation. As shown in Figure 3, the P-wave velocity increases with increasing axial stress, while Figure 4 demonstrates a concurrent increase in the effective P-wave quality factor. These observations indicate that the effective elastic stiffness increases, while attenuation decreases systematically during loading. The simultaneous increase in velocity and Q is consistent with progressive closure of compliant pores and microcracks, which enhances grain-contact stiffness and suppresses anelastic energy losses within the rock matrix.

The observed velocity-stress relationship is consistent with classical rock physics interpretations, according to which increasing axial stress progressively closes compliant pores and microcracks, leading to a nonlinear increase in elastic stiffness. While velocity primarily reflects the instantaneous stiffness of the load-bearing framework, attenuation is controlled by energy loss processes such as friction slip at grain contact points.

Overall, the presented results demonstrate that both ultrasonic velocity and attenuation exhibit systematic stress-dependent behavior in sandstone. While velocity

variations can be determined robustly from travel-time measurements, reliable estimation of the Q factor requires significantly greater attention to measurement stability, amplitude consistency, and spectral processing. Consequently, accurate attenuation characterization represents not only a petrophysical problem but also a critical measurement-technology challenge.

6. CONCLUSIONS

Ultrasonic pulse-transmission measurements under stepwise loading reveal pronounced pressure-dependent behavior in both P-wave velocity and Q in sandstone. Using an aluminum reference of identical geometry enables spectral-ratio-based separation of intrinsic rock attenuation from instrumental effects. These results provide laboratory evidence for path-dependent anelastic dissipation in stress-sensitive sedimentary rocks. By supplementing the field measurement results with laboratory measurements, we can obtain more accurate and robust results when determining individual rock physical parameters.

Since attenuation is particularly sensitive to irreversible or weakly reversible microstructural processes, it can provide additional information about stress-induced rock damage compared to velocity. To further investigate this, loading–unloading measurements and hysteresis tests incorporating quality factor (Q) analysis are required. Although hysteresis behavior has been examined previously (Dobróka and Somogyiné Molnár, 2012a), the present methodology enables direct estimation of attenuation through Q, offering enhanced sensitivity to microstructural changes. Thus, seismic attenuation provides information beyond the elastic modulus and serves as a sensitive indicator of microstructural evolution and internal friction in rocks (Toksöz and Johnston 1981; Tutuncu et al. 1994). The results therefore emphasize the potential value of temporal Q measurements as complementary indicators of stress evolution and rock damage.

From a broader geophysical perspective, laboratory observations of the stress dependence of velocity and attenuation have important implications for seismic monitoring of stress-sensitive environments such as reservoirs, fault zones, and geothermal systems. In this context, a better understanding of the stress-dependent properties of rocks can contribute to more efficient exploration and monitoring of geothermal systems and subsurface energy storage solutions, thereby supporting sustainable energy applications.

ACKNOWLEDGMENTS

This work was supported by the National Research, Development and Innovation Office (NKFIH), Hungary, through the National Research, Development and Innovation Fund under project ADVANCED-152958.

REFERENCES

Best, A. I. (1997). The effect of pressure on ultrasonic velocity and attenuation in near-surface sedimentary rocks. *Geophysical Prospecting*, 45, pp. 345–364. DOI: 10.1046/j.1365-2478.1997.00344.x

Birch, F. (1960). The velocity of compression waves in rocks to 10 kilobars. Part 1. *Journal of Geophysical Research*, 65, pp. 1083-1102. https://doi.org/10.1029/JZ065i004p01083

Darot, M., Reuschlé, T. (2000). Acoustic wave velocity and permeability evolution during pressure cycles on a thermally cracked granite. *International Journal of Rock Mechanics and Mining Sciences*, 37, pp. 1019–1026. https://doi.org/10.1016/S1365-1609(00)00034-4

Dobróka, M., and Somogyiné Molnár, J. (2012a). Kőzetfizikai modellezés akusztikus hiszterézis vizsgálatára. *Magyar Geofizika*. 53(2), pp. 73-79.

Dobróka, M., and Somogyi Molnár, J. (2012b). The pressure dependence of acoustic velocity and quality factor — New petrophysical models. Acta Geodaetica et Geophysica Hungarica, 47(2), pp. 149–160.

Hassan, A., and Vega, S. (2011). Fluid Content and Pore Type Effects on Acoustic Velocities in Carbonates. *73rd EAGE Conference*, Extended Abstract P152, https://doi.org/10.3997/2214-4609.20149478

He, T., and Schmitt, D. R. (2006). Velocity measurements of conglomerates and pressure sensitivity analysis of AVA response. *Proceedings of 76th SEG International Exposition and Annual Meeting*, New Orleans, USA

King, M. S. (2009). Recent developments in seismic rock physics. *International Journal of Rock Mechanics and Mining Sciences*, 46, pp. 1341–1348.

Mavko, G., Mukerji, T., and Dvorkin, J. (2009). *The Rock Physics Handbook* (2nd ed.), Cambridge University Press.

Meglis, I. L., Greenfield, R. J., Engelder, T., and Graham, E. K. (1996). Pressure dependence of velocity and attenuation and its relationship to crack closure in crystalline rocks. *Journal of Geophysical Research*, Solid Earth, 101(B8), pp. 17523–17532.

Nur, A. and Simmons, G. (1969). Stress-induced velocity anisotropy in rock. *Journal of Geophysical Research,* 74, pp. 6667-6674. https://doi.org/10.1029/JB074i027p06667

Sengun, N., Altindag, R., Demirdag, S., Yavuz, H. (2011). P-wave velocity and Schmidt rebound hardness value of rocks under uniaxial compressional loading. *International Journal of Rock Mechanics and Mining Sciences*, 48, pp. 693–696.

Stacey, T. R. (1976). Seismic assessment of rock masses. *Proceedings of the Symposium on Exploration for Rock Engineering*, Johannesburg, 2, pp. 113-117.

Toksöz, M. N., Johnston, D. H., and Timur, A. (1979). Attenuation of seismic waves in dry and saturated rocks, *Geophysics*, 44(4), pp. 681–690.

Toksöz, M. N., and Johnston, D. H. (1981). Seismic Wave Attenuation. *Society of Exploration Geophysicists*.

Tutuncu, A. N., Podio, A. L., and Sharma, M. M. (1994). Nonlinear ultrasonic velocity and attenuation in sedimentary rocks, *Geophysics*, 63 (1), pp. 195-203.

Wyllie, M. R. J., Gregory, A. R., Gardner, L. W. (1956). Elastic Wave Velocities in Heterogeneous and Porous Media. *Geophysics*, 21, pp. 41–70.

Wyllie, M. R. J., Gregory, A. R., Gardner, G. H. F. (1958). An experimental investigation of factors affecting elastic wave velocities in porous media. *Geophysics*, 23, pp. 459–493.

Zong, J., Stewart, R. R., and Dyaur, N. (2020). Attenuation of Rock Salt. Ultrasonic Lab Analysis of Gulf of Mexico Coastal Samples, *Journal of Geophysical Research*, Solid Earth, 125, e2019JB019025.